Neuroendocrinology Letters Volume 41 No. 7-8 2020
ISSN: 0172-780X; ISSN-L: 0172-780X; Electronic/Online ISSN: 2354-4716
Web of Knowledge / Web of Science: Neuroendocrinol Lett
Pub Med / Medline: Neuro Endocrinol Lett

ORIGINAL ARTICLE

Selective vulnerability of the hippocampus to the cytotoxic edema; magnetic resonance imaging and fluorescence microscopy studies in the rats

Petr Kozler[1], Vít Herynek[2], Dana Marešová[1], Pablo D. Perez[2], Luděk Šefc[2], Jaroslav Pokorný[1]

1 Institute of Physiology, First Faculty of Medicine, Charles University, Prague, Czech Republic
2 Center for Advanced Preclinical Imaging, First Faculty of Medicine, Charles University, Prague, Czech Republic

Correspondence to: Prof. MUDr. Jaroslav Pokorný, DrSc
Institute of Physiology, First Faculty of Medicine, Charles University
Albertov 5, Praha 2, 128 00
TEL.: +420224968416; E-MAIL: jaroslav.pokorny@lf1.cuni.cz

Submitted: 2020-11-02 Accepted: 2020-12-26 Published online: 2020-12-26

Key words: **Water intoxication; Cytotoxic edema; Vasogenic Edema; Magnetic resonance imaging; Fluorescence microscopy; Rats; Hippocampus; Cerebral cortex**

Neuroendocrinol Lett 2020; **41**(7-8):392–400 **PMID:** 33754596 NEL417820A08

Abstract

OBJECTIVES: Changes in the hippocampus induced by water intoxication were studied using fluorescence microscopy (FM) and magnetic resonance imaging (MRI).

METHODS: In three animals (rats), intracellular/extracellular distribution of Evans blue (EB) in cerebral cortex and hippocampus of both hemispheres was revealed by injection of EB into the internal carotid artery (ICA) in hyperhydrated rats (water intoxication, WI). A total of 8 experimental rats were used for the MRI study. The animals were scanned before WI, then the experimental brain edema was induced by WI and MR scanning was performed at day 1 and day 8 after WI. Besides standard T2-weighted imaging an apparent diffusion coefficient (ADC) and transverse relaxation time (T2) were evaluated.

RESULTS: Hyperhydration brought about the largest intracellular deposits of EB in CA3 hippocampal region, followed by the cerebral cortex and CA1 hippocampal region with the lowest amount of intracellular EB in the dentate gyrus. A higher apparent diffusion coefficient (corresponding to a vasogenic edema) was found the first day after hyperhydration in the cortex and in the CA1 and CA3 regions with no changes in dentate gyrus.

CONCLUSION: Both FM and MRI confirmed a selectively higher vulnerability to hyperhydration and hyponatremia (achieved by water intoxication) of the hippocampal cells compared to dentate gyrus cells.

Abbreviations &Units:

CA1	- cornu ammonis 1	MRI	- magnetic resonance imaging
CA3	- cornu ammonis 3	MR	- magnetic resonance
DG	- dentate gyrus	WI	- water intoxication
CCA	- common carotid artery	BBB	- blood-brain barrier
ECA	- external carotid artery	EB	- Evans Blue
ICA	- internal carotid artery	ADC	- apparent diffusion coefficient
MW	- molecular weight	T2	- transverse relaxation time of water protons

T2W MR image - T2-weighted magnetic resonance image
CG - control group
WI Day 1 - one day after edema induction
WI Day 8 - eight days after edema induction
CT - computed tomography
TBI - traumatic brain injury
FM - fluorescence microscopy
ICP - intracranial pressure
mmHg - millimeter of Mercury
mmol/l - millimoles per liter
g - gram
TE_{eff} - effective echo time
TR - repetition time
TF - turbo factor
NA - number of acquisitions
FOV - field of view

INTRODUCTION

For over 130 years, it has been known that pathologic insults, such as ischemia, hypoglycemia, oxidative stress, and anoxia, can cause structural damage to the hippocampus. The hippocampus respond to these pathologic conditions is heterogeneous with the cellular damage most clearly displayed in the CA1 region, whereas the dentate gyrus, CA3, and most cortical neurons appear to be more resistant. (Bartsch *et al.* 2015).

The selective vulnerability of the hippocampus has been extensively studied in experimental rat models, mainly in models of ischemia (Westerberg *et al.* 1987; Ouyang *et al.* 2007; Fan *et al.* 2008; Arvola *et al.* 2019). Selective changes in the hippocampus were described also after seizures (Sloviter, 1989) and TBI (Qian *et al.* 1996; Shepherd *et al.* 2003). Much less attention has been paid so far to hippocampal selective changes during brain edema (Kawamata *et al.* 2003). Due to its structural integrity and specific vulnerability, the neuronal population of the hippocampus is one of the most studied areas of the brain in experimental models of various pathological conditions.

In previous papers in this journal we demonstrated results of our study of the experimental brain edema induced by water intoxication (WI). Those experiments were based on various methods: light microscopy (Kozler *et al.* 2010; Kozler *et al.* 2011; Kozler & Pokorný, 2012), CT imaging (Kozler & Pokorný, 2014), electroencepalography (Marešová *et al.* 2014; Marešová *et al.* 2016), biochemical findings (Kozler *et al.* 2016), behavioural studies (Kozler *et al.* 2017a; Kozler *et al.* 2017b; Marešová *et al.* 2018), and intracranial pressure monitoring (Kozler *et al.* 2019; Kozler *et al.* 2020). We use the experimental model of water intoxication for its general and long-term recognized applicability in the induction of brain edema.

The present paper is aimed to compare the distribution of water in the intracellular/extracellular domain in the hippocampus in the model of an experimental brain edema (water intoxication), using fluorescence microscopy (FM) and magnetic resonance imaging (MRI). The choice of these two methods was intentional. Fluorescence microscopy belongs among basic research methods in the spectrum of experimental models while magnetic resonance imaging is a very sophisticated method of preclinical research. So comparing the results of these two different methods can bring a new aspect into the problem. We also used some methods of the FM experiment described in our previous study (Kozler & Pokorný, 2003).

MATERIAL AND METHODS

All experiments were approved by the Ethical Committee of the First Faculty of Medicine (Charles University in Prague) and were in agreement with the Guidelines of the Animal Protection Law of the Czech Republic and Guidelines for the treatment of laboratory animals EU Guidelines 86/609 / EEC. For experiments, male rats of the Wistar strain weighing 400-410 g (Velaz, Prague, Czech Republic).

Water intoxication

The distilled water (DW) in a total amount corresponding to 20 % of body weight was injected intraperitoneally (i.p.) in three consecutive doses over 24 h with simultaneous administration of desmopressin. Each sub-dose represented one third of the total dose 0.032 mg/kg (desmopressin (1-desamino-8-D-arginine vasopressin) (OCTOSTIM®, Ferring). Desmopressin is an antidiuretic hormone which potentiates the effect of hyperhydration by inducing hyponatremia (Yamaguchi *et al.* 1997 Silver *et al.* 1999, Manley *et al.* 2000, Vajda *et al.* 2000).

The fluorescence microscopy group

Transfer of Evans blue (EB) from the blood into microenvironment of cortex and hippocampus (Fig. 1) was studied in both hemispheres after EB injection into the internal carotid artery (ICA) of hyperhydrated rats by water intoxication.

Evans blue (EB, MW 961 Da) is an intravital tracer often used to test BBB permeability. The molecular weight (MW) of EB is so high that it does not allow the tracer to pass through the intact BBB (Wolman *et al.* 1981). We chose an intracarotic way of EB application so that the penetration of the tracer into the brain blood circulation was as fast as possible. The presence of EB in the brain thus proves a disruption of BBB. We used three animals in this group. For general anesthesia, each rat received 4 mg/100 g of thiopental applied intraperitoneally. Using the microsurgical technique, the right-sided common carotid artery (CCA), internal carotid artery (ICA) and external carotid artery (ECA) were exposed from a linear incision between the sternal manubrium and mandible. A polyethylene catheter fixed by ligation was introduced into the bifurcation through a small arteriotomy of the CCA. The rats had the ECA ligated close behind the bifurcation. All rats underwent standard water intoxication within 24 hours prior to EB administration (Olson

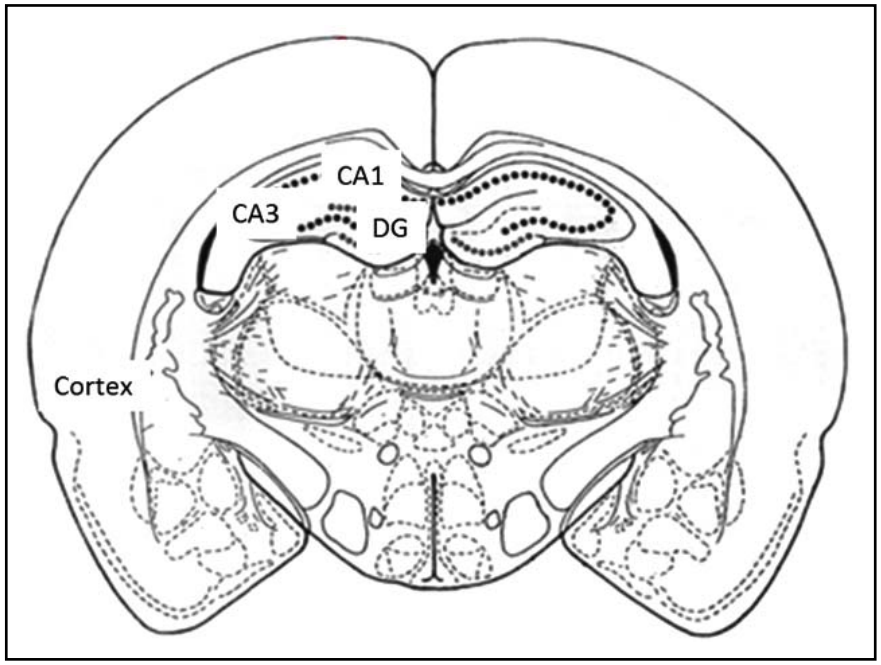

Fig. 1. Fluorescence microscopy group - evaluated areas
Legend: cortical and hippocampal cornu ammonis subfields CA1, CA3 and DG are depicted.

et al. 1994). 2 % EB at a dose of 2 ml/kg was applied into CCA catheter at a rate of 0.45 ml/min (Saris *et al.* 1988). After the application, the catheter was removed and the CCA ligated below and above the arteriotomy. The operation wound was closed in a single layer, and the spontaneously ventilating rat was placed in a heated box (37 °C). Within 30 min after the end of the surgery, the brain was fixed by transcardial perfusion with a 4% paraformaldehyde solution in pH 7.4 phosphate buffer for a period of 15 min, and then fixed in the same solution for another 24 h. Each brain was then sliced on a vibratome into coronary sections 30 μm thick and then, without further staining, placed on slides for microscopic examination. The sections were studied under a fluorescence microscope for intracellular and extracellular distribution of the EB in the cortex, in the CA1, CA3 areas and dentate gyrus (DG) of the hippocampus in both hemispheres. The ratio of intracellular/extracellular distribution of the EB in each area was expressed in per cent (e.g. the ratio 62.5%:37.5% represents the intracellular/extracellular distribution in the given area). The results represent the average of all the data obtained in three rats. As plasma natremia reflects the degree of hyperhydration, hyponatremia confirms osmotic cellular edema (Liang *et al.* 2007; Kozler & Pokorný, 2003). The respective blood samples were obtained from a catheter in the CCA before any of the applications.

The magnetic resonance imaging group

The aim of this experiment was to determine changes in the cortex and hippocampus after water intoxication by magnetic resonance imaging.

A total of 8 experimental animals were used. Whole group was subjected to MR scanning before water application (intact animals), one day after edema induction (24 hours after the last water dosage application – Day 1), and 8 days after (Day 8).

We selected the first day after WI to determine the distribution of water in the acute phase of brain edema. We chose the eighth day after WI according to the results of another study, in which myelin disorder persisted in the same time interval after WI (Kozler & Pokorny, 2012). The experimental question was whether there is a time correlate between structural and MRI changes.

Animals were anesthetized by spontaneous inhalation of isoflurane (Forane®, AbbVie Ltd.) in air (3% for induction, 1.5–2% for maintenance) during water intoxication and MR examinations.

MR scanning

MR imaging was performed using a 1 T MR scanner ICON (Bruker, Ettlingen, Germany). The imaging protocol included basic T2-weighted turbo-spin echo sequence in sagittal and/or coronal directions (effective echo time TE_{eff} = 60 ms, repetition time TR = 2500 ms, turbo factor TF = 16, number of acquisitions NA = 16, 14 slices, slice thickness 1 mm, field of view FOV = 30 × 30 mm^2, matrix 128 × 128), axial T2- weighted turbo-spin echo sequence with higher resolution (TE_{eff} = 60 ms, TR = 2500 ms, TF = 16, NA = 16, 14 slices, slice thickness 1 mm, FOV = 30 × 30 mm^2, matrix 256 × 256), CPMG sequence for T2-mapping (echo spacing TE = 7.79 ms, TR = 3600 ms, 7 slices, slice thickness 2 mm, FOV = 30 × 30 mm^2, matrix 128 × 128, NA = 2) and diffusion-weighted sequences (echo planar imaging

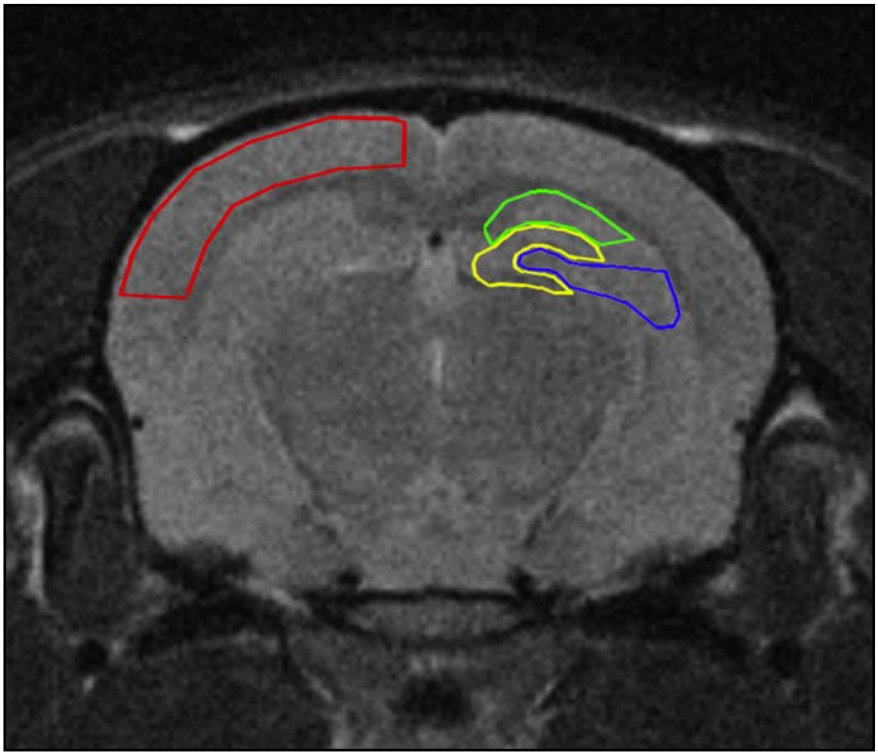

Fig. 2. Magnetic resonance imaging group - the rat brain with outlined evaluated areas. Legend: Red – cortex; green – hippocampus CA1 area; blue – hippocampus CA3 area; yellow – dentate gyrus (DG).

sequence, *TE*= 28 ms, *TR* = 3000 ms, *NA* = 8, diffusion gradient in read (left-right) direction, five *b*-values: 35, 225, 425, 82, 1625 s/mm^2, 9 slices, slice thickness 2 mm, *FOV* = 30 × 30 mm^2, matrix 64 × 64) for evaluation of ADC maps.

T2 and ADC maps were calculated using an in-house VIDI program (Herynek *et al.* 2012) written in Matlab (MathWorks, Natick, MA, USA). Relaxation times and diffusion coefficients were evaluated in the cortex and hippocampus in both hemispheres (Fig 2).

Differences were analyzed using an unpaired two-tailed t-test. $p < 0.05$ was considered as statistically significant.

RESULTS

The fluorescence microscopy group

The ratio of intra/extracellular EB distribution in the evaluated areas represented the average of all data obtained from both hemispheres in three rats (Fig. 3).

The EB distribution 30 minutes after tracer application to ICA in hyperhydrated rats is presented in Fig. 3. All rats underwent standard water intoxication within 24 hours prior to EB administration. The sodium blood value was 20 mmol/l lower than normal.

We considered the intracellular distribution of EB to be a real sign of the vulnerability of hippocampal cells. The presence of this high molecular weight tracer inside the cells indicates damage to the cytoplamatic membrane. Differences in the intracellular amount of EB (black columns in Fig. 3) were analyzed using an unpaired two-tailed t-test. $p < 0.05$ was considered as statistically significant. Results in Fig. 3 show a significantly larger intracellular amount of EB in CA3 compared to the intracellular amount of EB in DG. There were no significant differences in the intracellular amount of EB between Cortex, CA1 and DG.

The magnetic resonance imaging group

Typical T2W MR image and calculated T2 and ADC maps are shown in Figure 4.

Changes in ADC and T2 values in the cortex and hippocampus before and after WI are summarized in Figure 5 and Figure 6.

The ADC was higher after induction of edema (day 1) in the cortex and in the CA1 and CA3 regions. This corresponded to a vasogenic edema. After eight days the ADC values normalized. No changes of ADC were found in the DG. T2 values did not significantly change in any of the observed areas. This indicates the absence of cytotoxic edema.

DISCUSSION

The hippocampus is a bilaminar gray matter structure located medially in the temporal lobe that protrudes over the temporal horn of the lateral ventricle and occupies the medial region of its floor. The hippocampus

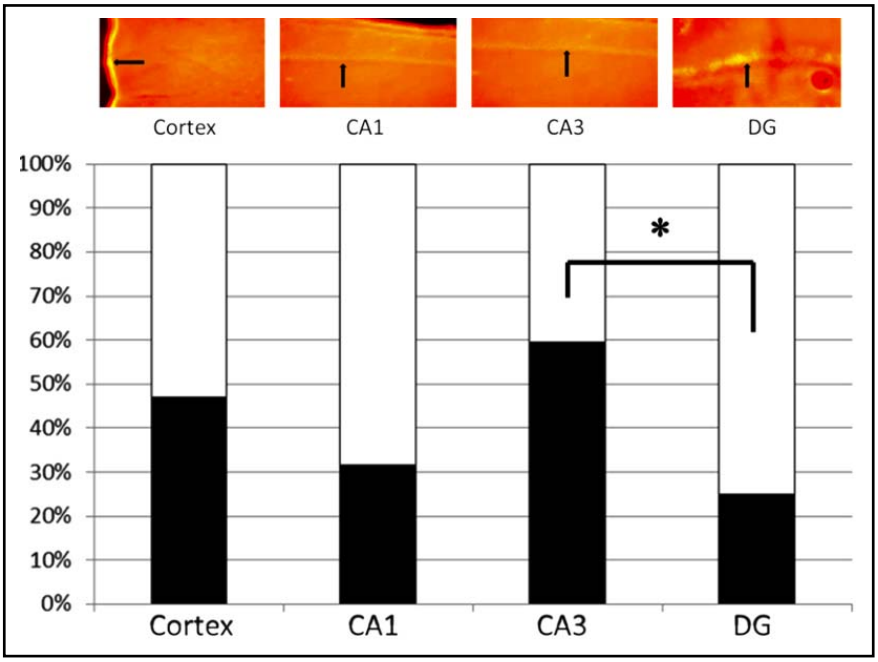

Fig. 3. Intracellular/extracellular ratio of Evans Blue distribution.
Legend: cortex, hippocampus CA1 area (CA1), hippocampus CA3 area (CA3), and dentate gyrus (DG). Black arrows indicate the fluorescence of intracellularly deposited EB.White columns: extracellular distribution of EB, black columns: intracellular distribution of EB. Intracellular/extracellular distribution ratio: Cortex – 47%/53%, CA1 – 31,5%/68,5%, CA3 – 59,5%/40,5%, DG – 25%/75%. Asterix marks a significantly larger intracellular amount of EB in CA3 compared to the intracellular amount of EB in DG. There were no significant differences in the intracellular amount of EB between Cortex, CA1 and DG.

consists of two interlocking gray matter folds, the cornu ammonis (or hippocampus proper) and the dentate gyrus. Based on its cellular composition, the cornu ammonis is divided into four parts, the so-called Sommer's sectors CA1 to CA4 (Amaral & Lavenex, 2006). The hippocampus plays an important role in spatial and episodic memory, and can be affected by a wide range of congenital variants and degenerative, inflammatory, vascular, tumoral and toxic-metabolic pathologies (Dekeyzer *et al.* 2017). The hippocampus responds to these pathologic conditions with a heterogeneous susceptibility: the cellular damage is most clearly displayed in the hippocampal CA1 region whereas the dentate gyrus, CA3, and most cortical neurons appear to be more resistant (Bartsch *et al.* 2015). The exact mechanisms of this region-specific selective vulnerability are not well understood but may include genomic-dependent glutamate and calcium-mediated mechanisms

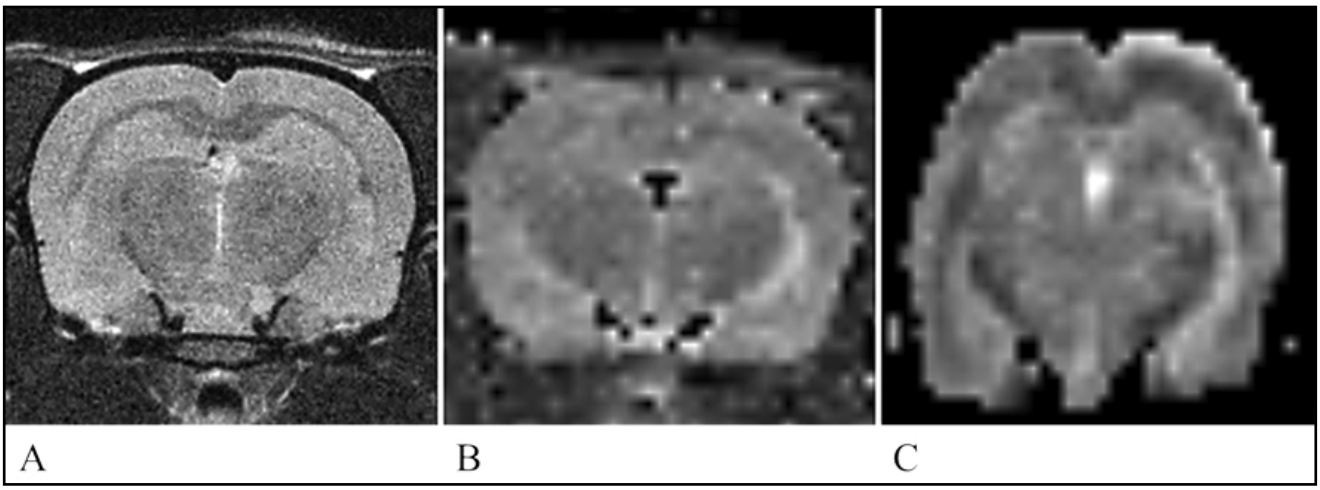

Fig. 4. A typical T2-weighted image, T2 map and ADC map.
Legend: A typical T2-weighted image (A) of the rat brain showing the evaluated slice. B – T2 map (interpolated), C – ADC map (interpolated). Note geometrical distortions of the ADC map caused by magnetic field inhomogeneities in combination with EPI k-space acquisition.

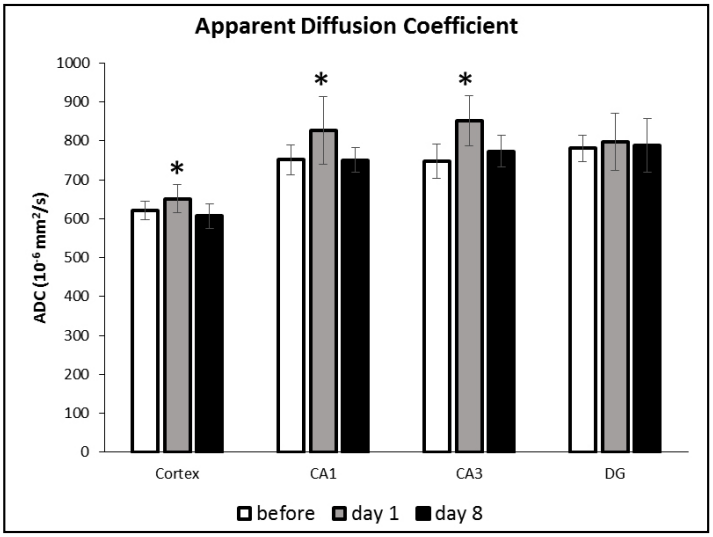

Fig. 5. ADC values in the selected regions.
Legend: cortex, hippocampus CA1 area (CA1), hippocampus CA3 area (CA3), and dentate gyrus (DG). Values were obtained before edema induction (white columns), on day 1 (grey) and day 8 (black) after edema induction. Asterix marks a significant increase of ADC compared to values before edema induction.

of neuronal excitotoxicity and oxidative stress as well as inflammatory changes (Wang & Michaelis, 2010). In experimental rat models, the selective vulnerability of CA1 to ischemia is quite well outlined. Probable causes may be the difference in arachidonic acid accumulation (Westerberg *et al.* 1987), loss of glutamate transport activity (Ouyang *et al.* 2007), reduction of the hyperpolarization-activated non-selective cationic current (Fan *et al.* 2008), and differences in microRNAs profiles (Arvola *et al.* 2019). Selective vulnerability of hippocampal neurons to seizure activity may be related to differences in the concentration of cytoplasmic proteins capable of sequestering free intracellular calcium (Sloviter, 1989). In experimental rat models of acute brain injury (fluid percussion injury), diffusion-weighted MRI demonstrated pathological swelling in CA1-CA3 cells, but not in DG cells (Qian *et al.* 1996, Shepherd *et al.* 2003). Kawamata *et al.* (2003) used a rat model of kaolin-induced hydrocephalus that led to an interstitial brain edema. The edema impaired oxidative metabolism and shifted the metabolism to anaerobic glycolysis with the impairment of glucose metabolism first observed in the CA3 region.

Brain edema is mainly classified into vasogenic edema and cytotoxic edema. Vasogenic edema is characterized by extravasation and extracellular accumulation of fluid into the cerebral parenchyma caused by disruption of the blood-brain barrier (BBB). In contrast, cytotoxic edema is characterized by intracellular accumulation of fluid and Na^+ resulting in cell swelling (Klatzo, 1967; Kimlberg, 1995; Liang *et al.* 2007; Michinaga & Koyama, 2015).

In this current study, we induced brain edema by water intoxication and detected cortical and hippocampal changes by fluorescence microscopy and MRI.

In the FM group, the presence of high molecular weight EB was evident in all evaluated cell populations. All rats in this experiment underwent standard water intoxication within 24 hours prior to EB administration. The presence of EB in the brain was made possible by water intoxication with hyperhydration and hyponatremia. These phenomena bring an osmotic imbalance at the cell membrane followed by intracellular flow of sodium and simultaneous accumulation of water. This primary effect initiates a cascade of processes leading to the subsequent increase of BBB permeability. The cascade includes: the loss of calcium and potassium homeostasis (Siesjo, 1993; Kimelberg, 1995; Barzó *et al.* 1997), release of excitotoxic amino acids (Bullock *et al.* 1994; Kimelberg, 1995; Barzó *et al.* 1997), release of free oxygen radicals (Kontos, 1989, Kimelberg, 1995, Barzó *et al.* 1997), and induction of intracerebral tissue acidosis (Siesjo *et al.* 1993, Kimelberg, 1995, Barzó *et al.* 1997).

Other observations showed that while the cytotoxic edema is characterized by intracellular accumulation of fluid, it makes the BBB more permeable (Lythgoe *et al.* 2000, Sorby-Adams *et al.* 2017).

We found (Fig. 3) significant larger intracellular amount of EB in CA3 compared to the intracellular amount of EB in DG. We considered the intracellular distribution of EB to be a real sign of the vulnerability of hippocampal cells. The presence of this high molecular weight tracer inside the cells indicates impairment to the cytoplasmic membrane. The selective vulnerability of the hippocampus due to brain edema is in accordance with the results published by Kawamata *et al.* (2003). We confirmed that the CA3 region is the most sensitive to hyperhydration and hyponatremia.

MRI represents a method of choice in clinical practice for diagnosis of suspected brain edema (Ho *et al.* 2012).

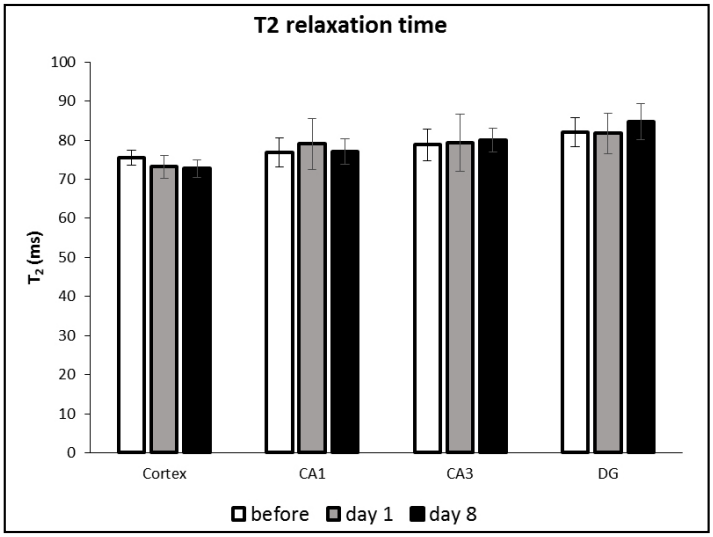

Fig. 6. T2 values in the selected regions.
Legend: cortex, hippocampus CA1 area (CA1), hippocampus CA3 area (CA3), and dentate gyrus (DG). Values were obtained before edema induction (white columns), on day 1 (grey) and day 8 (black) after edema induction.

Quantitation of apparent diffusion coefficient (ADC) or T2 relaxation time has been proposed as a supplemental measurement for more specific differential diagnostics in various diseases (Wagnerová *et al.* 2012), and is also suitable for investigation of an experimental brain edema (Michinaga & Koyama, 2015). Cytotoxic and vasogenic edema after brain injury can be differentiated by a combination of ADC and T2 imaging. Diffusion-weighted imaging provides information about the cellular architecture such as cellular size, membranes and volume fraction. ADC is an indicator of the magnitude of diffusion of water molecules within the tissue. ADC increases with higher extracellular volume and amount of fluids, and it is reduced when cell swelling is observed due to narrowing of the extracellular space within the cerebral parenchyma. T2 is related to water content and vascular permeability. In general, reduced ADC values correlate with a cytotoxic edema (and vice versa increased ADC values correlate with an experimental vasogenic edema). A cytotoxic edema represents mainly redistribution of water from extracellular to intracellular compartments; therefore, shrinkage of extracellular space leads to decrease of ADC. Increased T2 values reflect higher water content and may be observed during development of both vasogenic and cytotoxic edema, however changes in T2 relaxation times during transition from a vasogenic edema to a cytotoxic one may be ambiguous (Ito *et al.* 1996; Badaut *et al.* 2007). Moreover, ADC imaging has proved to be more sensitive than T2 imaging (Loubinoux *et al.* 1997).

We observed significantly increased ADC values on day 1 in the cortex and in the cornu amonis (subfields CA1 and CA3) corresponding to the vasogenic edema. The values were normalized after eight days, which corresponded rather to diminishing of the vasogenic edema, rather then to transition into a cytotoxic one. We did not find any changes to the ADC in dentate gyrus. T2 values did not change in any of the observed structures. This finding indicates that the cytotoxic edema was not developed. According to Sorby-Adams *et al.* (2017) a vasogenic edema occurs in the setting of BBB disruption due to cytotoxic edema and in time course follows this primary condition. In the absence of cytotoxic edema indicated by constant T2 values, this phenomenon explains the presence of vasogenic edema in the cortex and cornu ammonis.

The absence of vasogenic edema in DG confirms the selective vulnerability of hippocampal neuronal populations to hyperhydration and hyponatremia.

In our structural study, we demonstrated the presence of the disintegration of the myelin after WI (Kozler & Pokorny, 2012). Results of the study showed that cellular edema can bring myelin disintegration and that these changes are time dependent – the most serious degree of disintegration was found one week after the edema induction. Onaya (2002) on the basis of neuropathological studies proved that axonal disintegrity accompanying diffuse brain injuries is always preceded by cellular edema and he concluded that the occurrence of damaged axons is not possible without cellular edema. Axonal disintegrity was documented in the post-TBI period, when no signs of brain edema were present. His findings are consistent with our experience that structural lesions of myelin after WI last for a longer period than signs of an edema in MR images.

To conclude, we used fluorescence microscopy and magnetic resonance imaging to show changes in cortical and hippocampal neuronal populations after induction of a brain edema by water intoxication. Fluorescence microscopy confirmed that the largest intracellular

amount of EB distribution was in CA3, followed by cortex and CA1. The lowest amount of intracellular EB distribution was in dentate gyrus. Magnetic resonance showed increased ADC values on day 1 in the cortex and in the cornu amonis (subfields CA1 and CA3) corresponding to the vasogenic edema. We did not find any changes in the ADC in the dentate gyrus. Both the presence of high molecular weight EB in the brain and vasogenic edema indicate increased BBB permeability due to induced cytotoxic edema by water intoxication. Both fluorescence microscopy (method of basic research) and magnetic resonance imaging (method of preclinical or clinical research) confirm a selectively higher vulnerability to hyperhydration and hyponatremia (achieved by water intoxication) of cornu amonis cells compared to dentate gyrus cells.

In general, the results of the study brought new findings that may help reveal the dynamics of the conversion of different types of brain edema over time and thus provide a promising opportunity for targeted and adequate treatment.

CONFLICT OF INTEREST

The authors declare no conflict od interest.

ACKNOWLEDGEMENTS

Supported by Charles University, Prague, Czech Republic - grant Progres Q35/LF1), and by Ministry of Education, Youth and Sports of the Czech Republic - Czech-BioImaging LM2018129. The facility infrastructure was supported by European Regional Development Fund No. CZ.02.1.01/0.0/0.0/18_046/0016045 (OPVVV project).

REFERENCES

1 Amaral D, Lavenex P (2006). "Ch 3. Hippocampal Neuroanatomy". In Andersen P, Morris R, Amaral D, Bliss T, O'Keefe J (eds.). The Hippocampus Book. Oxford University Press.
2 Arvola O, Kaidonis G, Xu L, Griffiths B, Stary CM (2019). Hippocampal sub-regional differences in the microRNA response to forebrain ischemia. Mol Cell Neurosci. **98**: 164–178.
3 Badaut J, Ashwal S, Tone B, Regli L, Tian Hr, Obenaus A (2007). Temporal and regional evolution of aquaporin-4 expression and magnetic resonance imaging in a rat pup model of neonatal stroke. Pediatr Res. **62**: 248–254.
4 Bartsch T, Döhring J, Sigrid Reuter S, Carsten Finke C, Axel Rohr A, Henriette Brauer H, Günther Deuschl G, Olav Jansen O (2015). Selective neuronal vulnerability of human hippocampal CA1 neurons: lesion evolution, temporal course, and pattern of hippocampal damage in diffusion-weighted MR imaging. J Cereb Blood Flow Metab. **35**: 1836–1845.
5 Barzó P, Marmarou A, Fatouros P, Hayasaki K, Corwin F (1997). Contribution of vasogenic and cellular edema to traumatic brain swelling measured by diffusion-weighted imaging. J Neurosurg **87**: 900–907.
6 Bullock R, Zauner A, Tsuji O (1994). Excitatory amino acid release after severe human head trauma: effect of intracranial pressure and cerebral perfusion pressure changes. In: Intracranial Pressure IX. H Nagai, K Kamiya, S Ishii (eds), Springer, Tokyo, pp 264–267.
7 Dekeyzer S, Isabelle De Kock I, Nikoubashman O, Vanden Bossche S, Ruth Van Eetvelde R, De Groote J, Acou M, Wiesmann M, Deblaere K, Achten E (2017). Insights Imaging. **8**: 199–212.
8 Fan Y, Deng P, Wang YC, Lu HC, Xu ZC, Schulz PE (2008). Transient cerebral ischemia increases CA1 pyramidal neuron excitability. Exp Neurol. **212**: 415–421.
9 Herynek V, Wagnerová D, Hejlová I, Dezortová M, Hájek M (2012). Changes in the brain during long-term follow-up after liver transplantation. J Magn Reson Imaging. **35**: 1332–1337.
10 Ho ML, Rojas R, Eisenberg RL (2012). Cerebral Edema. AJR Am J Roentgenol. **199**(3): W258–W273, DOI: 10.2214/AJR.11.8081
11 Ito J, Marmarou A, Barzó P, Fatouros P, Crowin F (1996). Characterization of edema by diffusion-weighted imaging in experimental traumatic brain injury. J Neurosurg. **84**: 97–103.
12 Kawamata T, Katayama Y, Tsuji N, Nishimoto H (2003). Metabolic derangements in interstitial brain edema with preserved blood flow: selective vulnerability of the hippocampal CA3 region in rat hydrocephalus. Acta Neurochir Suppl. **86**: 545–547.
13 Kimelberg HK (1995). Current concepts of brain edema. Review of laboratory investigations. J Neurosurg. **83**: 1051–1059.
14 Klatzo I (1967). Presidential Address. Neuropathological aspects of brain edema. J Neuropathol Exp Physiol. **26**: 1–14.
15 Kontos HA (1989). Oxygen radicals in CNS damage. Chem Biol Interact **72**: 229–255.
16 Kozler P, Pokorný J (2003). Altered Blood-Brain Barrier Permeability and Its Effect on the Distribution of Evans Blue and Sodium Fluorescein in the Rat Brain Applied by Intracarotid Injection. Physiol Res. **52**: 607–614.
17 Kozler P, Riljak V, Pokorny J (2010). Time-dependent axonal impairment in experimental model of brain oedema. Neuro Endocrinol Lett. **31**: 477–482.
18 Kozler P, Riljak V, Pokorný J (2011). Methylprednisolone reduces axonal impairment in the experimental model of brain oedema. Neuro Endocrinol Lett. **32**: 831–835.
19 Kozler P, Pokorny J (2012). Effect of methylprednisolone on the axonal impairment accompanying cellular brain oedema induced by water intoxication in rats. Neuro Endocrinol Lett. **33**: 782–786.
20 Kozler P, Pokorny J (2014). CT density decrease in water intoxication rat model of brain oedema. Neuro Endocrinol Lett. **35**: 608–612.
21 Kozler P, Sobek O, Pokorny J (2016). Biochemical manifestations of the nervous tissue degradation after the blood-brain barrier opening or water intoxication in rats. Neuro Endocrinol Lett. **37**: 114–120.
22 Kozler P, Maresova D, Pokorny J (2017a). An experimental model of the "dual diagnosis": Effect of cytotoxic brain edema plus peripheral neuropathy on the spontaneous locomotor activity of rats. Neuro Endocrinol Lett. **38**: 408–414.
23 Kozler P, Maresova D, Pokorny J (2017b). Study of locomotion, rearing and grooming activity after single and/or concomitant lesions of central and peripheral nervous system in rats. Neuro Endocrinol Lett. **38**: 495–501.
24 Kozler P, Maresova D, Pokorny J (2018) Cellular brain edema induced by water intoxication in rat experimental model. Neuro Endocrinol Lett. **39**: 209–218.
25 Kozler P, Maresova D, Pokorny J (2019). Cytotoxic brain edema induced by water intoxication and vasogenic brain edema induced by osmotic BBB disruption lead to distinct pattern of ICP elevation during telemetric monitoring in freely moving rats. Neuro Endocrinol Lett. **40**: 249–256.
26 Kozler P, Maresova D, Pokorny J (2020). Intracranial pressure and mean arterial pressure monitoring in freely moving rats via telemetry; pilot study. Neuro Endocrinol Lett. **40**: 319–324
27 Liang D, Bhatta S, Gerzanich V, Simard JM (2007). Cytotoxic edema: mechanisms of pathological cell swelling. Neurosurg Focus. **15**: E2
28 Loubinoux I, Volk A, Borredon J, Guirimand S, Tiffon B, Seylaz J, Méric P (1997). Spreading of vasogenic edema and cytotoxic edema assessed by quantitative diffusion and T2 magnetic resonance imaging. Stroke. **28**: 419–426.

29 Lythgoe MF, Thomas DL, Calamante F, Pell GS, King MD, Busza AL, et al (2000). Acute changes in MRI diffusion, perfusion, T(1), and T(2) in a rat model of oligemia produced by partial occlusion of the middle cerebral artery. Magn Reson Med. **44**: 706–712.
30 Manley GT, Fujimura M, Ma T, Noshita N, Filiz F, Bollen AW, et al (2000). Aquaporin-4 deletion in mice reduces brain edema after acute water intoxication and ischemic stroke. Nat Med. **6**: 159–163.
31 Maresova D, Kozler P, Pokorny J (2014). Neuronal excitability after water intoxication in young rats. Neuro Endocrinol Lett. **35**: 274–279.
32 Maresova D, Kozler P, Pokorny J (2016). Neuronal excitability changes depend on the time course of cellular edema induced by water intoxication in young rats. Neuro Endocrinol Lett. **37**: 207–212.
33 Maresova D, Kozler P, Miletínová E, Zima T, Pokorny J (2018). Locomotion in young rats with induced brain cellular edema - effects of recombinant human erythropoietin. Neuro Endocrinol Lett. **39**: 310–314.
34 Michinaga S, Koyama Y (2015). Pathogenesis of brain edema and investigation into anti-edema drugs. Int J Mol Sci. **16**: 9949–9975.
35 Olson JE, Evers JA, Banks M (1994). Brain osmolyte content and blood-brain barrier water permeability surface area product in osmotic edema. Acta Neurochir **60** (Suppl): 571–573.
36 Onaya M (2002). Neuropathological investigation of cerebral
37 white matter lesions caused by closed head injury. Neuropathology. **22**: 243–251
38 Ouyang YB, Voloboueva LA, Xu LJ, Giffard RG (2007). Selective dysfunction of hippocampal CA1 astrocytes contributes to delayed neuronal damage after transient forebrain ischemia. J Neurosci. **27**: 4253–4260.
39 Qian L, Nagaoka T, Ohno K, Tominaga B, Nariai T, Hirakawa K, Kuroiwa T, Takakuda K, Miyairi H (1996). Magnetic resonance imaging and pathologic studies on lateral fluid percussion injury as a model of focal brain injury in rats. Bull Tokyo Med Dent Univ. **43**: 53–66.
40 Saris SC, Wright DC, Oldfield EH, Blasberg RC (1988). Intravascular streaming and variable delivery to brain following carotid artery infusions in the Sprague-Dawley rat. J Cereb Blood Flow Metab. **8**: 116–120.
41 Sorby-Adams AJ, Marcoionni AM, Dempsey ER, Woenig JA, Turner RJ (2017). The Role of Neurogenic Inflammation in Blood-Brain Barrier Disruption and Development of Cerebral Oedema Following Acute Central Nervous System (CNS) Injury. Int J Mol Sci. **18**: E1788.
42 Schmidt-Kastner R, Freund TF (1991). Selective vulnerability of the hippocampus in brain ischemia. Neuroscience. **40**: 599–636
43 Shepherd TM, Thelwall PE, Blackband SJ, Pike BR, Hayes RL, Wirth ED 3rd (2003). Diffusion magnetic resonance imaging study of a rat hippocampal slice model for acute brain injury. J Cereb Blood Flow Metab. **23**: 1461–1470.
44 Siesjo BK, Katsura K, Mellegard P (1993). Acidosis-related brain damage. Prog Brain Res. **96**: 23–48.
45 Silver SM, Schroeder BM, Bernstein P, Sterns RH (1999). Brain adaptation to acute hyponatremia in young rats. Am J Physiol. **276**: R1595–1599.
46 Sloviter RS (1989). Calcium-binding protein (calbindin-D28k) and parvalbumin immunocytochemistry: localization in the rat hippocampus with specific reference to the selective vulnerability of hippocampal neurons to seizure aktivity. J Comp Neurol. **280**: 183–196.
47 Vajda Z, Promeneur D, Dóczi T, Sulyok E, Frøkiaer J, Ottersen OP, Nielsen S (2000). Increased aquaporin-4 immunoreactivity in rat brain in response to systemic hyponatremia. Biochem Biophys Res Commun. **270**: 495–503.
48 Wagnerová D, Herynek V, Malucelli A, Dezortová M, Vymazal J, Urgošík D, et al (2012). Quantitative MR imaging and spectroscopy of brain tumours: a step forward? Eur Radiol. **22**: 2307–2318.
49 Wang X, Michaelis EK (2010). Selective Neuronal Vulnerability to Oxidative Stress in the Brain. Front Aging Neurosci. **2**: 12.
50 Westerberg E, Deshpande JK, Wieloch T (1987). Regional differences in arachidonic acid release in rat hippocampal CA1 and CA3 regions during cerebral ischemia. J Cereb Blood Flow Metab. **7**: 189–192.
51 Wolman M, Klatzo I, Chui E, Wilmes F, Nishimoto K, Fujiwara K, Spatz M (1981). Evaluation of the dyeprotein tracers in pathophysiology of the blood-brain barrier. Acta Neuropathol. **54**: 55–61.
52 Yamaguchi M, Yamada T, Kinoshita I, Wu S, Nagashima T, Tamaki N (1997). Impaired learning of active avoidance in water-intoxicated rats. Acta Neurochir Suppl. **70**: 152–154